JOURNAL OF GEOPHYSICAL RESEARCH, VOL. 102, NO. B5, PAGES 9961–9981, MAY 10, 1997

Global plate velocities from the Global Positioning System

Kristine M. Larson

Department of Aerospace Engineering Sciences, University of Colorado, Boulder

Jeffrey T. Freymueller

Geophysical Institute, University of Alaska, Fairbanks

Steven Philipsen

Department of Aerospace Engineering Sciences, University of Colorado, Boulder

Abstract.
We have analyzed 204 days of Global Positioning System (GPS) data from the global GPS network spanning January 1991 through March 1996. On the basis of these GPS coordinate solutions, we have estimated velocities for 38 sites, mostly located on the interiors of the Africa, Antarctica, Australia, Eurasia, Nazca, North America, Pacific, and South America plates. The uncertainties of the horizontal velocity components range from 1.2 to 5.0 mm/yr. With the exception of sites on the Pacific and Nazca plates, the GPS velocities agree with absolute plate model predictions within 95% confidence. For most of the sites in North America, Antarctica, and Eurasia, the agreement is better than 2 mm/yr. We find no persuasive evidence for significant vertical motions (< 3 standard deviations), except at four sites. Three of these four were sites constrained to geodetic reference frame velocities. The GPS velocities were then used to estimate angular velocities for eight tectonic plates. Absolute angular velocities derived from the GPS data agree with the no net rotation (NNR) NUVEL-1A model within 95% confidence except for the Pacific plate. Our pole of rotation for the Pacific plate lies 11.5° west of the NNR NUVEL-1A pole, with an angular speed 10% faster. Our relative angular velocities agree with NUVEL-1A except for some involving the Pacific plate. While our Pacific-North America angular velocity differs significantly from NUVEL-1A, our model and NUVEL-1A predict very small differences in relative motion along the Pacific-North America plate boundary itself. Our Pacific-Australia and Pacific-Eurasia angular velocities are significantly faster than NUVEL-1A, predicting more rapid convergence at these two plate boundaries. Along the East Pacific Rise, our Pacific-Nazca angular velocity agrees in both rate and azimuth with NUVEL-1A.

Introduction

For almost 20 years, models of current plate motions have been determined using spreading rates at mid-ocean ridges, transform fault azimuths, and plate boundary earthquake slip vectors [*LePichon*, 1968; *Chase*, 1972; *Minster et al.*, 1974; *Minster and Jordan*, 1978; *Chase*, 1978; *DeMets et al.*, 1990]. With the exception of earthquake slip vectors, these data represent an average over a substantial period of time (for the NUVEL-1 model of *DeMets et al.*[1990], the last 3.16 m.y.). These models have been tremendously successful in explaining the large-scale features of plate kinematics. Global plate models have shown plate interiors to be rigid over geologic timescales. The various geologic data all give consistent measures of global plate motions, although earthquake slip vectors have been found to be biased in some cases due to the partition of slip at certain margins where subduction occurs obliquely [*DeMets et al.*, 1990; *Argus and Gordon*, 1990]. Absolute plate motions have been computed based on the NUVEL-1 relative plate motions and the assumption of no net rotation (no net torque on the lithosphere), resulting in the absolute motion model no net rotation (NNR) NUVEL-1 [*Argus and Gordon*, 1991]. A recent revision of the magnetic time scale led to the rescaled NUVEL-1 models, NUVEL-1A

Paper number 97JB00514.
0148-0227/97/97JB-00514$09.00

and NNR NUVEL-1A (hereinafter referred to as NNR-A) [*DeMets et al.*, 1994].

Space geodetic data collected over the last two decades have made it possible to measure plate motions over the time scale of years rather than millions of years [e.g., *Robbins et al.*, 1993]. The ability to make global-scale geodetic measurements was made possible through the development of highly sophisticated space geodetic techniques such as satellite laser ranging (SLR) and very long baseline interferometry (VLBI). One of the primary scientific goals when these techniques were being developed was to measure global plate motions. Both SLR and VLBI achieved sufficient accuracy that they could be used to measure both global plate motions and plate boundary deformation [*Clark et al.*, 1987; *Smith et al.*, 1990; *Robbins et al.*, 1993; *Ryan et al.*, 1993], but both suffered from the disadvantage of the high cost and nonportability of the systems, which limited the number and distribution of sites worldwide. At roughly the same time SLR and VLBI were being developed and tested, the Department of Defense began deployment of the Global Positioning System (GPS). Its primary mission was and is to provide real-time navigation and positioning assistance. Scientists quickly realized that GPS could also be used for positioning with a precision approaching that of VLBI and SLR. GPS analysis softwares has been developed over the past decade for this purpose [e.g. *Dong and Bock*, 1989; *Beutler et al.*, 1987; *Blewitt*, 1989]. The GPS constellation has now been completed and a global tracking network is operating under international cooperation. The focus of this paper will be to use GPS and the global tracking network to study plate tectonics.

Why is geodetic analysis of global plate motions important when geologic models have been so successful? Geodetic techniques have become increasingly prominent in studies of plate boundary deformation and have approached the level of precision of global plate models. Geodetic techniques also measure plate motion over a period of a few years rather than a few million years, so it is important to find discrepancies that would indicate if there have been any very recent changes in plate motions. Today, regional tectonic studies in California and elsewhere are attempting to characterize fault slip rates in plate boundary zones so completely that the entire slip budget compares to a global plate model to within a few millimeters per year or better. Such studies are only feasible if the rates of plate motions are known to the same level of precision and if the rates of motion over the last few years (or few hundred years) are described adequately by a plate motion model averaged over the last few million years. Early space geodetic studies have shown a high correlation between observed relative site velocities and the predictions of the NUVEL-1 model [*Smith et al.*, 1990]. In this study we will compare angular velocities for eight plates and various plate pairs derived from our GPS data with the NUVEL-1A model. This study differs from the similar work of *Argus and Heflin* [1995] by including more sites, more tectonic plates, and a longer time series and by using only a subset of the available GPS data. This allows us to analyze the entire data set using the same models and techniques. We also include selected temporary occupations of sites rather than restricting ourselves to only permanent station data, improving the distribution of sites on some of the plates.

Measurements

While some global GPS tracking sites have existed since the late 1980s, the operation and archiving of the network were not globally coordinated, and the distribution of stations was too sparse to support global GPS studies. This changed in January-February 1991 with the International Association of Geodesy (IAG) sponsored global GPS densification experiment, the first Global International Earth Rotation Service (IERS) and Geodynamics campaign (hereinafter referred to as GIG). Over 100 GPS receivers were deployed in this campaign, although many were of insufficient quality to be truly useful [*Melbourne et al.*, 1993]. Analysis of a subset of the GIG data provided direct evidence of the potential of global GPS: 1 cm positioning accuracy [*Blewitt et al.*, 1992] and submilliarcsecond pole position estimates [*Herring et al.*, 1991]. Following the success of GIG, the IAG sponsored the development of the International GPS Service for Geodynamics (IGS), which provides timely access to high-accuracy GPS ephemerides based on data from a global network of permanent GPS receivers. The IGS has coordinated development of the global GPS network, which is now generally referred to as the IGS network.

Data from sites participating in the IGS network are downloaded by the agencies which operate them, and transferred via internet to the IGS global data centers. The number of GPS receivers participating in the IGS network continues to expand. At present, there are more than 70 global sites in the IGS network, excluding dense regional clusters in California. The most significant change over the last few years has been the increase in the number of IGS sites in the southern hemisphere, from four in 1992 to more than 5 times that number today. Receiver, antenna, and software descriptions for the IGS network are documented at the IGS Central Bureau (http://igscb.jpl.nasa.gov).

For this paper, we have analyzed data for the period between January 1991 and March 1996. The sites we have chosen for this study are listed in Table 1 and shown in Figure 1. Of these 38 sites, 16 were first observed during the 3 week GIG campaign. There is then a 1 year gap in our time series, until enough permanent stations had been deployed for the IGS network. Beginning in March 1992, we have analyzed data from the IGS network on a weekly basis. An analysis of IGS data from January 1991 through November 1993 was previously presented by *Larson and Freymueller* [1995]. In

Table 1. Station Description

Site	Name[a]	IGS	Plate	Longitude, deg	Latitude, deg	First Epoch	Last Epoch	Total Epochs
1	Albert Head	ALBH	NOAM	236.513	48.201	1992.37	1996.25	161
2	Algonquin	ALGO	NOAM	281.929	45.765	1991.06	1996.25	200
3	Baltra Island[b]	BALT	NAZC	269.741	−0.461	1991.08	1996.25	9
4	Bermuda	BRMU	NOAM	295.304	32.198	1993.26	1996.25	125
5	Canberra	CANB	AUST	148.980	−35.220	1991.06	1996.25	181
6	Chatham Island	CHAT	PCFC	183.434	−43.766	1992.91	1996.25	16
7	Easter Island	EISL	NAZC	250.617	−26.994	1994.07	1996.25	48
8	Fairbanks	FAIR	NOAM	212.501	64.832	1991.06	1996.25	199
9	Fortaleza	FORT	SOAM	321.574	−3.852	1993.46	1996.25	123
10	Hartebeestoek	HART	AFRC	27.708	−25.738	1991.06	1995.99	188
11	Hobart[c]	HOBA	AUST	147.440	−42.614	1993.20	1995.96	92
12	Hercmonceaux	HERS	EURA	0.336	50.681	1992.17	1996.25	143
13	Kourou	KOUR	SOAM	307.194	5.218	1992.88	1996.25	130
14	Kootwijk	KOSG	EURA	5.810	51.994	1991.06	1996.25	192
15	Kokee Park	KOKB	PCFC	200.335	21.994	1991.06	1996.25	173
16	Mas Palomas	MASP	AFRC	344.367	27.607	1992.51	1995.99	157
17	Matera, Italy	MATE	EURA	16.704	40.461	1992.27	1995.99	131
18	Madrid, Spain	MADR	EURA	355.750	40.241	1991.06	1996.25	199
19	McMurdo[d]	MCM3	ANTA	166.675	−77.770	1991.06	1996.25	164
20	North Liberty	NLIB	NOAM	268.425	41.582	1993.20	1996.25	94
21	Ny Alesund[e]	NYAL	EURA	11.865	78.858	1991.08	1996.25	63
22	O'Higgins[f]	OHIG	ANTA	302.100	−63.168	1991.06	1995.88	37
23	Onsala	ONSA	EURA	11.926	57.222	1992.17	1996.25	180
24	Pamatai	PAMA	PCFC	210.425	−17.457	1992.17	1996.24	106
25	Pie Town	PIE1	NOAM	251.881	34.124	1993.00	1996.25	71
26	Penticton	PENT	NOAM	240.375	49.134	1992.17	1996.25	179
27	Perth	PERT	AUST	115.885	−31.632	1993.77	1996.25	78
28	Richmond	RCM5	NOAM	279.616	25.466	1992.57	1996.25	134
29	Santiago	SANT	SOAM	289.331	−32.976	1991.06	1996.25	198
30	St John's	STJO	NOAM	307.322	47.405	1992.41	1996.25	157
31	Taiwan	TAIW	EURA	121.537	24.876	1992.37	1996.25	162
32	Tromso	TROM	EURA	18.938	69.538	1992.17	1996.25	111
33	Townsville	TOWN	AUST	146.814	−19.141	1991.06	1992.88	45
34	Tsukuba	TSKB	EURA	140.088	36.106	1993.96	1996.25	59
35	Westford	WES2	NOAM	288.507	42.424	1993.21	1996.25	82
36	Wettzell	WETT	EURA	12.879	48.956	1991.06	1996.25	191
37	Wellington	WELL	AUST	174.783	−41.086	1991.06	1995.13	61
38	Yaragadee	YAR1	AUST	115.347	−28.885	1991.06	1996.25	204

[a]Unless stated otherwise, the local surveys between different monuments at the same site were taken from ITRF94 [*Boucher et al.*, 1996] or the IGS Central Bureau (http://igscb.jpl.nasa.gov).

[b]The 1996 observations were made at Isla Santa Cruz (GALA). Tie calculated for This paper: GALA minus BALT −4,973.763 , 404.838 , −31,181.929 m.

[c]Tie calculated for this paper: HOB2 minus HOBA 112.719, 50.737, −50.183 m.

[d]There are observations at four McMurdo monuments, defined as follows. McMurdo GIG: MCM1; McMurdo 1992–1993: MCM2; McMurdo 1994: MCM3; McMurdo 1995–1996: MCM4. Ties calculated for This paper: MCM1 minus MCM3 −234.600, 17.358, 52.521 m; MCM2 minus MCM3 −73.423, 54.691, 36.920 m; MCM4 minus MCM3 −1,081.537, 400.997, 145.126 m.

[e]Data from 1991–1992 excluded "The antenna had been hit by a stone... and was knocked over lying on its side," IGS Mail 135. No tie available between 1991–1992 location and 1993–1996 location.

[f]Tie from GIG site and permanent site, personnal communication, Andreas Reinhold: OHIG-GIG (K4) minus OHIG (K5): 4.715, −0.277, 0.849 m.

that paper, a global set of stations was analyzed, but only the velocities of sites on the Pacific, Australian, and Antarctic plates were discussed in detail. In this study, we have expanded our analysis and interpretation to include the Eurasian, North American, African, Nazca and South American plates.

Even though IGS data are available on a daily basis, we have chosen to analyze only one day of GPS data per week, except for special periods of interest such as the GIG campaign. Our decision is based on two characteristics of GPS data. First, it has been shown that GPS estimates are highly correlated over periods of several days [*King et al.*, 1995]. Thus, if solutions are computed each day, they will not be independent. Second, station velocity uncertainties are more sensitive to the time spanned by the data set than additional data points spaced closely together in time. In order to analyze as uniform as possible a data set and in an effort to

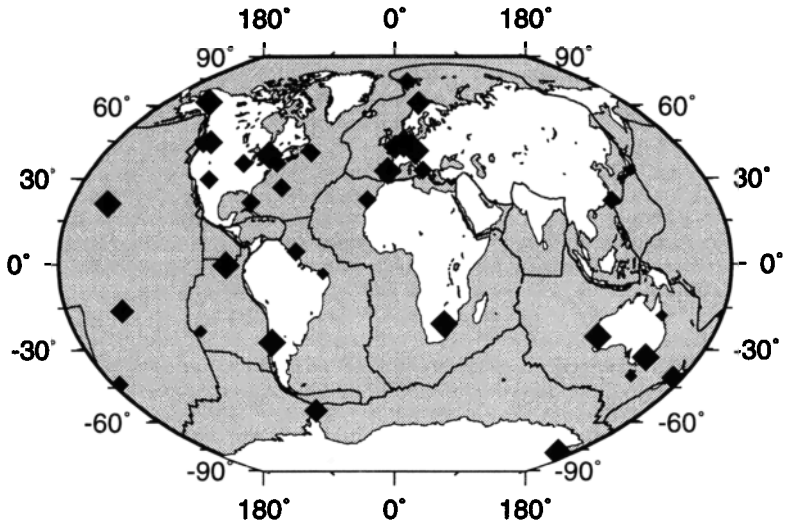

Figure 1. GPS stations used in this study. The size of the symbols correspond to the length of the time series, from more than 5 years, between 4 and 5 years, between 3 and 4 years, and less than 3 years.

avoid correlated estimates, we analyzed global tracking data only once per week. By restricting ourselves to a data set of manageable size, we have made it possible to reanalyze as much data as needed to ensure consistency of our solutions over time as modeling techniques have improved. Although we have analyzed more than the 38 sites in Table 1, we computed velocities only for the sites for which we feel an accurate and reliable velocity can be estimated. Therefore we excluded all sites with less than 2 years of data. Unfortunately, this means that we do not discuss some of the newest IGS sites in interesting tectonic areas such as central Asia. We also excluded data from sites that have been displaced by earthquakes. In addition to uncertainty associated with the coseismic deformation, these sites may also be affected by postseismic deformation. As a result, we do not discuss several of the long-term IGS sites in southern California.

Data Analysis

All data presented in this paper were analyzed using the GIPSY/OASIS II software (release 3 and release 4) developed at the Jet Propulsion Laboratory, California Institute of Technology. The current version of the software is an evolution of the software described by *Lichten and Border* [1987].

GIPSY uses undifferenced carrier phase and pseudorange observables. For a general description of the GPS observables and data analysis, see, for example, *Hofmann-Wellenhof et al.* [1993] and *Leick* [1995]. The carrier phase is more precise than the pseudorange but is ambiguous by an integer number of wavelengths so a carrier phase ambiguity must be estimated for each continuous phase-connected arc of GPS carrier phase data. The pseudorange is unambiguous but has a noise level approximately 100 times higher than the carrier phase. The pseudorange data are acquired by correlation of a code in the data signal, called the Pcode. During periods when the Pcode is encrypted (antispoofing, or AS), all modern receivers can extract equivalent pseudorange data from the signals by using signal crosscorrelation or other methods which tend to result in some degradation in signal to noise ratio and data quality. This varies by receiver type and local environment and has lessened over time as GPS receivers have been improved. We choose standard data weights of 1 cm for the carrier phase data and, with a few exceptions, 100 cm for the pseudorange data if the receiver records it. Pseudorange data from Rogue SNR-8 and Mini-Rogue SNR-800 receivers are biased under AS, so we excluded these pseudorange data during periods of AS (AS has been on almost continuously since January 30, 1994). Pseudorange data are also excluded from certain Turborogue SNR-8000 receivers that show pseudorange biases under AS.

All raw data were passed through an automatic editing stage, during which cycle slips (discontinuities in the phase data) were found and corrected and outliers were removed. For Rogue and Turborogue receivers, the TurboEdit algorithm [Blewitt, 1990] was used. For all other receivers, the PhasEdit algorithm (J. Freymueller, unpublished algorithm, 1996) was used. Both algorithms search for discontinuities in undifferenced geometry-free (and clock-free) linear combinations of the observables. After data editing, the data from both GPS frequencies are combined to form the ionosphere-free linear combination [see, e.g., *Leick*, 1995] and are decimated to a standard 6 min interval. Additional editing of the data is done manually based on inspection of postfit data residuals, and data can be deleted or new phase ambiguity parameters inserted when outliers or cycle slips are found to have passed undetected through the automated editing. The number of such editing changes re-

quired has varied somewhat with time. In general, prior to the introduction of AS almost all data problems were detected and corrected by the automatic algorithms. Data quality worsened considerably after the introduction of AS and has been improving steadily since then as the receiver hardware has been improved.

Parameter estimation in GIPSY is carried out using a Square Root Information Filter (SRIF) algorithm [*Bierman*, 1977] which allows us to estimate parameters as constants or varying in time. We estimate both station and satellite clock errors relative to a user-specified reference clock as white noise parameters, uncorrelated from epoch to epoch. We estimate the wet tropospheric path delay at zenith as a time-dependent parameter with a random walk noise model [*Lichten and Border*, 1987; *Tralli et al.*, 1988]. Orbits are modeled by integrating the equations of motion and estimating corrections to the initial conditions, as described by *Lichten and Border* [1987]. We estimate solar radiation pressure coefficients for the ROCK4 or ROCK42 model as appropriate [*Fliegel et al.*, 1992]. We estimate a single X-Z solar radiation pressure scale parameter, plus small independent X and Z corrections, and a Y-bias parameter. For satellites that are eclipsing (passing through Earths shadow on each revolution), we estimate time-varying solar radiation pressure parameters. The GPS yaw attitude model is described by *Bar-Sever* [1996].

A summary of the models used in GIPSY/OASIS and our parameter estimation strategy is given in Table 2. Each station position estimate is based on 24 hours of GPS data. We followed a strategy similar to that described by *Heflin et al.* [1992]. The coordinates of six globally distributed sites were constrained to agree with VLBI/SLR coordinates with an a priori uncertainty of 10 m. The remaining sites were constrained with an a priori uncertainty of 1 km. These loose constraints are sufficient to avoid singularities in the GPS solutions but are not sufficient to specify the reference frame.

We have made a considerable effort to analyze the entire time series of data consistently. The same models and strategies are used throughout, which has meant reanalyzing the earlier data as models have improved. Through this effort we hope to avoid aliasing systematic errors into our estimated station velocities and tectonic interpretations. There is one unavoidable difference between data collected in 1991-1993 and data collected in 1994-1996. On January 30, 1994, antispoofing was implemented on the GPS constellation. As described above, this reduced the quality of the carrier phase data and the amount of pseudorange data which was available to us. However, we have not been able to identify any significant changes in velocity which correlate with the introduction of AS.

Reference Frame

As described above, we estimate GPS station coordinates for each day of data in loosely constrained solu-

Table 2. Data Analysis Summary

Models	Value
Data interval	6 min
Elevation angle cut-off	15°
Geopotential	JGM3 degree and order 12
Precession	IAU 1976 precession theory
Nutation	IAU 1980 nutation theory
Earth Orientation	IERS bulletin B
Difference phase center correction	*Schupler and Clark* [1991]
Yaw attitude	*Bar-Sever* [1996]
Reference clock	Algonquin
Pseudorange weight	100 mm
Carrier phase weight	10 mm

Parameter	Estimation	Standard Deviation
Satellite position	force model	1 km
Satellite velocity	force model	0.00001 km/s
Satellite clock	white noise	1 s
Solar pressure Ybias	constant	10^{-12} km $s^{-1}s^{-1}$
Solar pressure X/Z	constant	1% of Ybias
Eclipsing satellites	stochastic	1 hour updates
Station position, reference	constant	0.01 km
Station position, nonreference	constant	1 km
Station clock	white noise	1 s
Phase ambiguity (real-valued)	constant	0.1 km
Zenith troposphere delay	random walk	10 mm/sqrt(hour)

tions. That means that we tightly constrained neither the coordinates of the tracking sites nor the orbits of the GPS satellites (see Table 2 for a description of our analysis strategy and constraint definitions). In our solutions, the orbits of the GPS satellites are not in a well-determined reference frame. The entire GPS constellation can be rotated in longitude without degrading the fit of the data to our models. Equivalently, the longitudes of our estimated station coordinates can be rotated without degrading the data fit, although this is not true for either height or latitude. However, while the entire GPS network and GPS constellation can be transformed as a rigid unit, our loosely constrained solutions still determine relative frame-invariant quantities very precisely. Station geocentric heights and baseline lengths are determined very precisely in the loosely constrained solutions, subject to some uncertainty in scale.

In order to use the coordinates derived from these solutions, we need to transform all of the loosely constrained solutions into a consistent reference frame so that we can derive rates of site motion (and plate motion) from the time series of coordinates. The reference frame defines the scale, origin, and orientation of our geodetic coordinates. The reference frame is specified by means of a priori information about the coordinates and/or velocities of sites, or other similar quantities. Since all plates on the Earth are moving, we must use a kinematic reference frame, that is, one which includes the time evolution of the reference frame parameters.

A reference frame is realized through the coordinates and covariances of individual stations. A seven parameter transformation can be estimated to transform an unconstrained GPS solution into a specific reference frame. The quality of the transformation will depend on the accuracy of the coordinates and velocities of the reference stations which are used to derive the transformation and on the geographic distribution of those stations. In addition to random errors in coordinates and velocities, the accuracy of the reference station coordinates can be compromised by errors in local survey ties.

For this study we have adopted the ITRF94 reference frame (International Terrestrial Reference Frame 1994 [*Boucher et al.*, 1996]). This is the best fit model of positions for 240 geodetic sites using the VLBI, SLR, GPS, and DORIS techniques. Velocities for some of the sites are also incorporated into ITRF94 if there are sufficient data to determine an accurate velocity estimate. In practice, ITRF94 velocities are available for sites with long histories of VLBI and SLR measurements. ITRF94 closely follows the development of previous frames, in particular, ITRF92 [*Boucher et al.*, 1993] and ITRF93 [*Boucher et al.*, 1994], with improvements both in data quality and estimation strategy. ITRF94 is designed to agree on average with the NNR-A absolute plate motion model, so ITRF94 velocities of sites on plate interiors should be directly comparable to the predictions of NNR-A if the plates are rigid.

We can transform our solutions into ITRF94 in different ways. *Larson and Freymueller* [1995] estimated a seven parameter transformation for each GPS solution and then simultaneously estimated linear fits to all sites using the entire time series. Unfortunately, this technique is sensitive to data outages at the reference sites. Owing to unavoidable random or systematic errors in the reference site coordinates and velocities, a different set of reference sites will produce a different realization of the reference frame. In this study we have applied the reference frame constraints differently. We first estimate the velocity and epoch position of each site from the unconstrained solutions, using the full covariance information from our GPS solutions. This velocity solution is, like the individual GPS solutions, loosely constrained. We then apply reference frame constraints by using the published ITRF94 positions and velocities for selected reference sites as pseudo-observations, weighted by the ITRF94 covariance matrix.

The reference sites we have chosen are listed in Table 3, and their locations are plotted in Figure 2. These were chosen for their (1) high accuracy, (2) geographic distribution, and (3) inclusion in the time series from 1991 through 1996. For geometric reasons, we would like to add a site in east Asia, but there were no sites that met our criteria for the period 1991-1996. There are many other sites in Europe and North America that could have been chosen, but these sites are close together and provide no additional geometric strength. We do not want to constrain the velocities of too many sites, because our objective is to study the tectonic implications of the GPS velocities.

Site Velocities

Using the techniques described above, we estimated velocities for 38 GPS sites. Velocity estimates, transformed into horizontal and vertical components, are listed in Table 4 along with the NNR-A velocity prediction and ITRF94 velocity, if available. This velocity solution is based on our entire time series of data.

It is instructive to compare the velocity estimates based on all of the data with an individual time series of coordinates derived from the same solutions by transforming each individual solution into the ITRF94

Table 3. Reference Stations

Site	Name	Location
1	Yaragadee	Australia
2	Santiago	South America-Nazca
3	Hartebeestoek	Africa
4	Madrid	Europe
5	Kokee Park	Pacific
6	Algonquin	North America
7	Fairbanks	North America

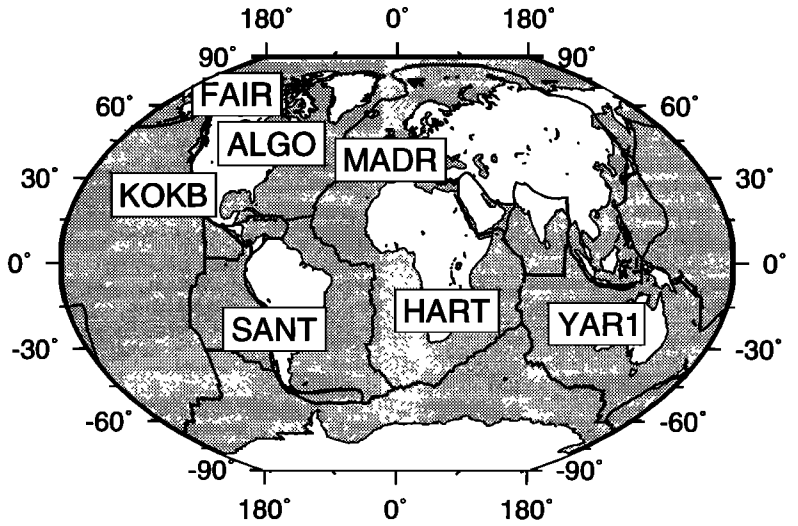

Figure 2. Stations used to define the reference frame (see Table 1 for station identifications).

Table 4. Station Velocities and Standard Deviations

	GPS			NNR-A		ITRF94		
Station	North	East	Up	North	East	North	East	Up
ALGO	2.6±1.2	−16.1±1.2	4.5±1.2	3.2	−17.0	1.0±1.4	−16.5±1.4	4.6±1.4
ALBH	−7.1±1.5	−6.0±1.6	−0.9±2.0	−14.0	−14.2			
BALT	9.2±1.9	41.7±5.0	−21.2±8.6	9.6	61.7			
BRMU	8.0±2.0	−13.4±2.2	−1.3±2.9	8.3	−12.3			
CANB	55.6±1.3	17.3±1.5	8.4±1.8	53.7	17.7	53.6 ± 2.2	21.4 ± 2.2	−1.6 ± 2.2
CHAT	38.4±2.0	−48.3±2.5	1.5±4.4	31.4	−40.5			
EISL	−4.9±2.9	77.4±4.2	−4.7±6.6	−8.9	79.4	−12.0 ± 2.2	75.1±2.3	−1.0 ± 2.2
FAIR	−21.6±1.2	−9.8±1.2	−1.6±1.2	−20.2	−10.3	−22.9 ± 1.5	−8.2 ± 1.6	−2.5 ± 1.5
FORT	10.1±2.1	-9.0±2.5	5.0±3.6	11.7	−5.5			
HART	16.9±1.3	16.6±1.3	−0.2±1.3	20.1	20.7	15.2 ± 2.1	16.2 ± 2.3	−1.6 ± 2.4
HERS	15.1±1.5	16.3±1.6	−1.6±2.2	15.2	17.6	15.9 ± 1.3	18.0 ± 1.5	1.9 ± 1.3
HOBA	55.4±2.2	16.2±2.5	5.4±3.5	54.4	12.8			
KOKB	33.4±1.2	−61.4±1.2	−0.3±1.2	32.3	−58.3	33.4 ± 1.7	−60.0 ± 1.6	−1.0 ± 1.5
KOSG	15.7±1.2	19.7±1.3	−4.9±1.7	14.5	18.5	15.3 ± 1.5	18.6 ± 1.9	−1.1 ± 1.5
KOUR	11.8±1.8	-4.4±2.1	0.1±3.1	11.1	−5.9			
MADR	15.7±1.2	20.2±1.2	2.9±1.2	15.7	18.6	16.1±1.4	18.7±1.5	1.9±1.4
MASP	17.7±1.7	16.6±1.9	1.3±2.5	17.5	17.1			
MATE	18.9±1.6	23.9±1.8	−4.8±2.3	12.8	22.0	18.0 ± 1.7	23.4±1.5	−2.4±1.6
MCM3	−10.5±1.4	8.7±1.5	−1.9±2.3	−11.7	7.5			
NLIB	−2.5±1.9	−16.2±2.1	0.0±2.7	−2.2	−15.9	−2.5 ± 2.7	−14.6 ± 1.8	−13.5 ± 2.8
NYAL	14.0±2.1	15.0±2.2	9.9±4.6	13.6	12.9			
OHIG	11.8±1.7	15.3±1.9	−7.4±3.1	10.2	16.3			
ONSA	14.4±1.5	18.0±1.6	0.7±2.0	13.6	18.6	13.0±1.5	17.9±1.6	−1.1 ± 1.5
PAMA	32.8±1.6	−74.8 ± 2.6	−1.5±3.5	31.5	−62.9			
PENT	−10.5±1.5	−14.6±1.6	−2.4±1.9	12.7	−15.1			
PERT	55.5±2.4	41.3±2.7	7.6±3.9	59.2	38.0			
PIE1	−8.2±1.8	−14.6±2.1	6.6±3.0	−8.7	−12.8			
RCM5	2.0±1.6	−12.7±1.8	−0.5±2.4	2.2	−10.7	3.3 ± 1.4	−8.9±1.4	1.7±1.2
SANT	17.5±1.3	17.2±1.3	5.4±1.3	9.5	−0.9	20.2±2.8	18.4±3.2	3.0 ± 2.8
STJO	14.6±1.6	−16.2±1.7	−2.4±2.0	12.6	−14.8			
TAIW	−12.8±1.6	27.1±2.1	−6.2±2.6	−13.3	22.3			
TOWN	56.5±3.3	23.3±4.2	19.3±7.2	54.7	30.0			
TROM	16.0±1.3	16.4±1.4	1.5±2.1	12.4	17.2	15.6±1.8	16.4±1.9	−0.3±2.0
TSKB	−16.6±2.6	−10.8±3.2	−1.9±4.2	15.7	−19.2			
WELL	34.4±1.7	−19.4±2.2	8.3±3.2	37.1	−0.6			
WES2	3.1±1.9	−15.6±2.1	−0.4±2.7	5.7	−15.7			
WETT	14.8±1.2	22.1±1.3	−2.0±1.8	13.5	20.3	14.2 ± 1.2	19.7 ± 1.4	−3.3 ± 1.3
YAR1	56.5 ± 1.2	38.4±1.2	6.2±1.2	59.1	39.0	58.4±1.4	38.5±1.4	4.2±1.3

In millimeters per year.

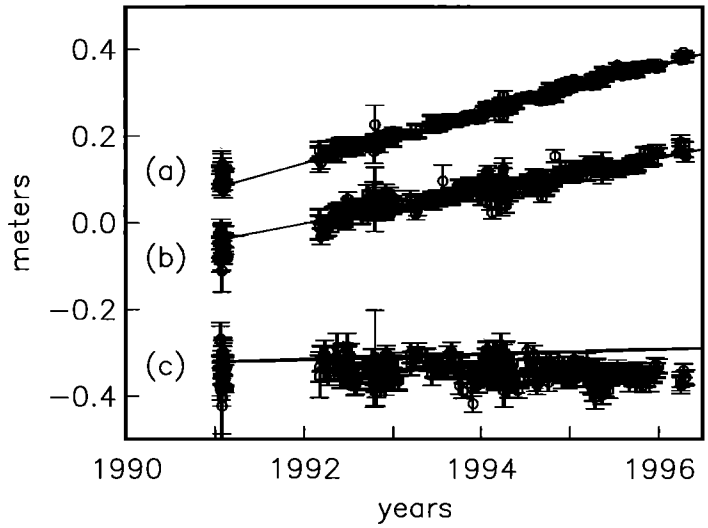

Figure 3. Individual epoch solutions in latitude, longitude, and height for Yaragadee, Australia. At each epoch, a seven-parameter transformation has been estimated between the unconstrained solutions and International Terrestrial Reference Frame 1994 [*Boucher et al.*, 1996]. Formal errors are one standard deviation. The lines shown are the fits to the global GPS solutions, as described in the text.

reference frame independently. The most frequently observed site in this study is Yaragadee (YAR1), located in western Australia. The latitude, longitude, and height estimates of this site as a function of time are shown in Figure 3 along with the linear fit of the global solution to the individual epoch solutions. The weighted RMS deviation about the best fit line is 4.5, 7.6, and 12.2 mm for latitude, longitude, and height, respectively. In Figure 4, we show a typical site from the northern hemisphere, Kootwijk (KOSG), located in the Netherlands. For Kootwijk, the weighted RMS deviation about the best fit line is 3.7, 4.9, and 9.4 mm for latitude, longitude, and height, respectively. The improvement in position standard deviation for both Kootwijk and Yaragadee from 1991 to the present is due to the increase in the number of satellites in the GPS constellation, from 15 satellites in 1991 to 24 today. The contrast in precision between Yaragadee and

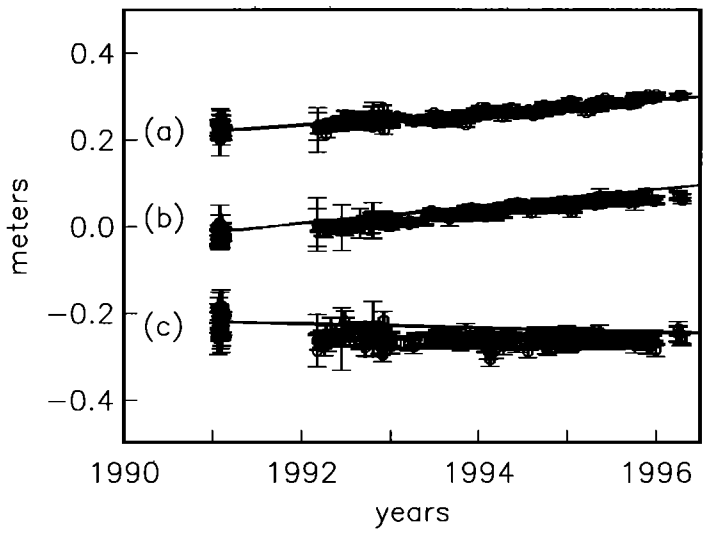

Figure 4. Individual epoch solutions in latitude, longitude, and height for Kootwijk, Netherlands. At each epoch, a seven-parameter transformation has been estimated between the unconstrained solutions and International Terrestrial Reference Frame 1994 [*Boucher et al.*, 1996]. Formal errors are one standard deviation. The lines shown are the fits to the global GPS solutions, as described in the text. Note that the Kootwijk coordinates are more precise when compared to Yaragadee in Figure 3. This is due to the strength of the IGS network in the northern hemisphere relative to the southern hemisphere.

Kootwijk reflects the greater number of tracking sites (and better realization of the ITRF) in the northern hemisphere relative to the southern hemisphere.

It is crucial that we properly estimate the uncertainties in our velocity estimates. It has long been known that the formal errors derived by GIPSY using the analysis strategy described in Table 2 underpredict the true scatter, or repeatability, of individual estimates. We have therefore scaled the position variances so that the reduced chi squared statistic of the velocity solution is approximately 1; this results in a variance scaling factor of 9. This scale does not compensate for systematic reference frame biases, possible non-Gaussian errors, or possible correlations between solutions. The assumption of uncorrelated data may be optimistic, since there is growing evidence for temporal correlations in GPS solutions. *King et al.* [1995] determined autocorrelations for a 10 km GPS baseline using a 384 day time series of data and found nonzero correlations for time lags up to 20 days, although the autocorrelations for all components were 0.1 or less for a time lag greater than 10 days. Long-term geodetic monument instability is another potential source of correlations between our solutions. *Langbein and Johnson* [1997] have analyzed a long time series of data from two-color laser line length measurements in California and found clear evidence for long-term correlations in line length measurements that can be described by a random walk process. Based on a similar length time series for a regional network in southern California, *Bock* [1995] suggests that a reasonable random walk variance would be of order 1 mm^2/yr, although there can be considerable variation from site to site depending on the local conditions and the way the GPS antenna is attached to the ground. However, *Herring* [1996] has suggested that these GPS time series are too short to determine whether a random walk error model is required. The significance of these results for the interpretation of geodetic time series has not yet been answered and is still an area of active debate.

Choosing a conservative approach, we increased our scaled uncertainties by additive factors to compensate for the possible effects of reference frame biases and correlations in the data. Our reference frame realization is not unique, and the geometry of the chosen reference stations is dictated by availability rather than optimal geographic distribution. If we vary the set of reference sites, we can produce small changes in our estimated velocities. We estimate that an additional site velocity uncertainty of 0.5 mm/yr is sufficient to characterize the possible systematic biases caused by a particular choice of reference sites. To address long-term correlations in the data, we follow the approach of Argus and Gordon [1996] and add a time-dependent velocity error, which decreases as the length of the time series increases. We modify the velocity variance as follows:

$$\sigma^2_{new} = \sigma^2_{formal} + \frac{C^2}{\Delta t^2} + \sigma^2_{frame} \qquad (1)$$

where $\sigma_{frame} = 0.5$ mm/yr, Δt is in years, and $C = 5.5$ mm, corresponding to the upper bound additive error suggested for VLBI data by *Argus and Gordon* [1996]. The σ^2_{formal} is the GIPSY variance multiplied by 9, as discussed earlier. We consider this to be a safe, conservative estimate of the uncertainties. In effect, for sites present throughout the entire time series, the two additive errors add 1.44 mm^2/yr^2 to the variance of each velocity component, so none of our velocities will have an uncertainty lower than about 1.2 mm/yr. Note that for sites present throughout the entire time series, the additive factors are larger than the scaled uncertainties based on random errors. We assume that the additive errors are uncorrelated from site to site.

The velocity estimates and their adjusted covariance are then used to estimate angular velocities for eight tectonic plates: Africa, Antarctica, Australia, Eurasia, Nazca, North America, Pacific, and South America. The three-dimensional velocity v of a geodetic site on any plate can be written as

$$v = \omega \times r \qquad (2)$$

where ω is the angular velocity of the plate and r is the position of the site (all Cartesian vectors). In the plate tectonic model, all station velocities are explicitly horizontal. The vertical component of the site velocity thus contributes nothing to the estimation of the angular velocity, so there are in reality only two data per station. With three parameters per angular velocity, velocities from two sites are required to determine all components of the angular velocity of a plate. A priori information can be applied to estimate an under-determined angular velocity, but in this paper we only estimated angular velocities for plates with at least two sites on them. The relative angular velocity for a plate pair is simply the difference of the absolute angular velocities for the two independent plates. Angular velocities are frequently expressed in terms of their pole of rotation and angular speed, and we follow that convention in this paper.

Geodetic Results

In this section we discuss the velocities of individual sites, and the discrepancies with respect to NNR-A (Table 4). Differences between our estimated velocities for most sites in the plate interiors and the NNR-A predictions are quite small worldwide, indicating that our reference frame is aligned with NNR-A. Differences at individual sites could be due to real differences in plate motions, local tectonic motions or site instability. In this study we have ignored effects due to postglacial rebound, although there have been observations of postglacial rebound from a longer time series of VLBI data [*Argus*, 1996] The effect due to postglacial rebound is primarily in the vertical component and we model the horizontal velocities exclusively.

Table 5. Plate Angular Velocities

Source	Angular Velocity: Latitude, deg,	Longitude, deg,	ω, deg/m.y.	Pole Error Ellipse: σ_{max}, deg	σ_{min}, deg	ψ, deg	σ_ω, deg/m.y.
			Africa (Hartebeestoek, Maspalomas)				
This paper	50.0	−86.8	0.26	5.3	2.8	90	0.01
NNR-A	50.8	−74.0	0.29				
			Antarctica (McMurdo and O'Higgins)				
This paper	60.5	−125.7	0.24	6.6	3.6	1	0.03
NNR-A	63.1	−115.9	0.24				
			Australia (Perth, Yaragadee, Canberra, Hobart, Townsville)				
This paper	31.4	40.7	0.61	3.1	1.0	-61	0.01
NNR-A	34.0	33.2	0.65				
			Europe (Hersmonceaux, Onsala, Tromso, Ny Alesund, Madrid, Kootwijk, Wetzell)				
This paper	56.3	−102.8	0.26	5.7	1.7	43	0.02
NNR-A	50.8	−112.4	0.23				
			Nazca (Baltra Island and Easter Island)				
This paper	40.6	−100.7	0.70	7.6	1.7	-5	0.05
NNR-A	48.0	−100.2	0.74				
			North America (Bermuda, North Liberty, Westford, Richmond, Algonquin, Fairbanks, St John's)				
This paper	−0.4	−84.5	0.22	4.3	2.0	0	0.01
NNR-A	−2.5	−86.0	0.21				
			Pacific (Pamatai, Kokee Park, Chatham)				
This paper	−63.1	95.9	0.70	2.3	0.9	−82	0.01
NNR-A	−63.2	107.4	0.64				
			South America (Kourou and Fortaleza)				
This paper	−21.0	−183.5	0.16	29.6	7.4	−71	0.06
NNR-A	−25.6	−124.0	0.12				

One sigma error ellipses are specified by the angular lengths of the principal axes and by the azimuths (ψ, given in degrees clockwise from north) of the major axis. The rotation rate uncertainty is determined from a one-dimensional marginal distribution [*DeMets et al.*, 1990, Table 2a].

We also discuss the estimated angular velocity for each plate (see Table 5). We first discuss the plates for which we have more than two sites with long time histories, as these are the best determined. Along with the angular velocities and their uncertainties, Table 5 lists the sites used to define each plate. In some cases, stations that were used as reference sites were also used to define the plate. It should be noted that while ITRF94 incorporates information from NNR-A, ITRF94 velocities are in many cases distinct from NNR-A predictions, and one of our reference sites is not located in a stable plate interior. For plates that include one of our reference sites, we carefully examine the pole fits to ensure that our results are not biased by the inclusion of reference sites. For example, the North American angular velocity is based on the velocities of seven sites, of which two, Algonquin and Fairbanks, are reference sites. If we remove Algonquin and Fairbanks, the estimated pole of rotation changes by 1.7° in latitude and 0.3° in longitude, and the maximum pole uncertainty increases from 4.3° to 7.9°. The change in the estimate of the angular velocity is much smaller than the uncertainty, so we conclude that the inclusion of the reference sites does not bias our estimate. The increase in standard error is caused by the geometry of the sites, meaning that Fairbanks is an important site for the estimation of the North America angular velocity. We followed a similar procedure for Madrid and the estimation of the Eurasia angular velocity and found a 30% increase in standard deviation when Madrid is removed. Only in the case of the African plate are our pole estimates strongly dependent on the assumed velocity of a reference site.

Eurasia

All of our sites on the stable Eurasia plate are located in western Europe. These sites all have long time series, as they were established as permanent sites in 1992 and many were also observed during GIG. Site velocities and residuals with respect to NNR-A are shown in Figure 5. All sites in the plate interior except Tromso agree with NNR-A velocities within 3 mm/yr and are well within 95% confidence limits. The discrepancy at Tromso appears to be real, as our estimate agrees with an independent analysis of GPS data for that site [*Boucher et al.*, 1996]. Matera, Italy, is located in the plate boundary zone between Eurasia and Africa, and thus we do not expect it to agree with NNR-A. Our velocity (18.9±1.6 mm/yr north and 23.9±1.8 mm/yr east) agrees well with the SLR measurements (18.0±1.7 mm/yr north and 23.4±1.5 mm/yr east) reported in ITRF94.

Our velocity for Taiwan is surprisingly close to that predicted for the stable Eurasian plate, even though it is located within a plate boundary zone (Figure 6).

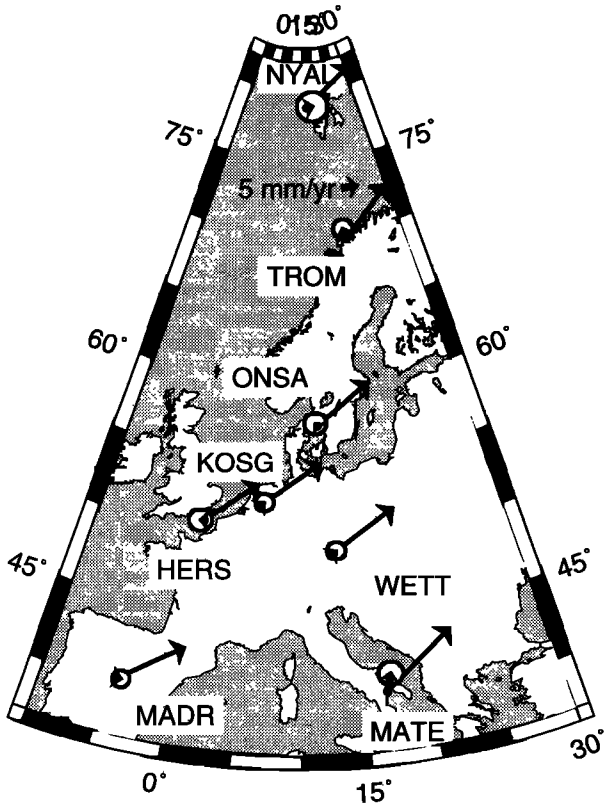

Figure 5. GPS station velocity estimates and NNR-A residuals for the Eurasia plate. The 95% confidence regions are shown attached to the residuals.

Molnar and Gipson [1996] presented VLBI results from Shanghai, about 800 km to the north of Taiwan, which show that south China is moving 8 ± 0.5 mm/yr at N116°E±4.1° with respect to the Eurasia plate. Our estimated velocity for Taiwan relative to the Eurasian plate is 4.8±2.0 mm/yr at N96°E, about 40% slower. The westward motion of Taiwan relative to Shanghai presumably is due to elastic deformation caused by the collision of the Philippine Sea plate with Eurasia.

Our estimate of the Eurasia angular velocity agrees with NNR-A within 95% confidence, but the uncertainty in our estimate is large. In order to reduce the uncertainty, we need a better distribution of sites within the plate rather than more precise velocities for sites in western Europe. For example, if each of the European sites used for our angular velocity estimate had a standard deviation of 1 mm/yr, the maximum pole position uncertainty would be 4.8° (with the actual data it is 6.3°). With the addition of an equally precise site in eastern Eurasia, the maximum pole position uncertainty would be reduced to 2.5°. An accurate velocity from one of the new IGS sites in Moscow would provide a similar improvement.

North America

We have good geometric coverage of the North American plate, with seven sites in the plate interior ranging from Alaska to Bermuda. We have also included Albert Head (British Columbia), Penticton (British, Columbia), and Pie Town (New Mexico) in our analysis of North America, although we have not assumed they are on the stable interior of the North American plate. The site velocities and residual velocities relative to NNR-A are shown in Figure 7. Fairbanks has a marginally significant southward velocity relative to NNR-A (2.1±1.1 mm/yr), consistent with VLBI. Of the three sites we removed from our angular velocity estimate, only Albert Head shows significant motion relative to North America, 11.4±1.6 mm/yr at N56°W, in

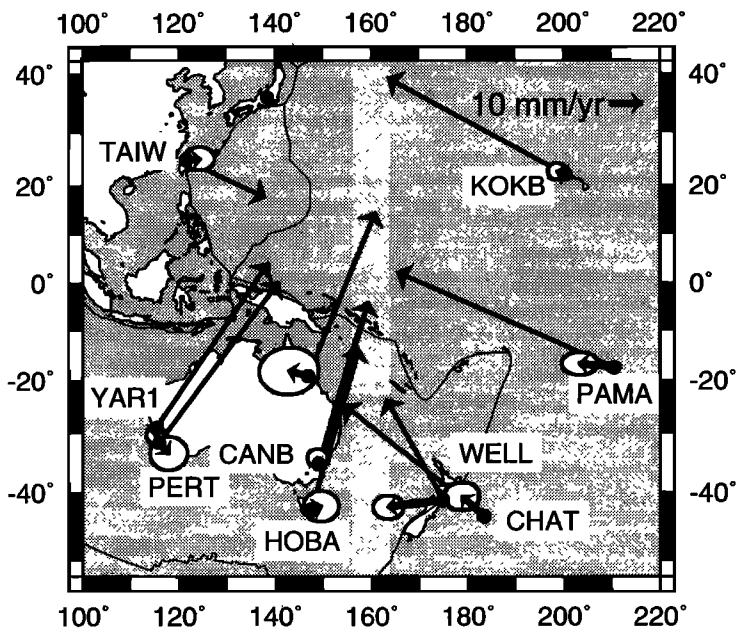

Figure 6. GPS station velocity estimates and NNR-A residuals for the Australia and Pacific plates. The 95% confidence regions are shown attached to the residuals.

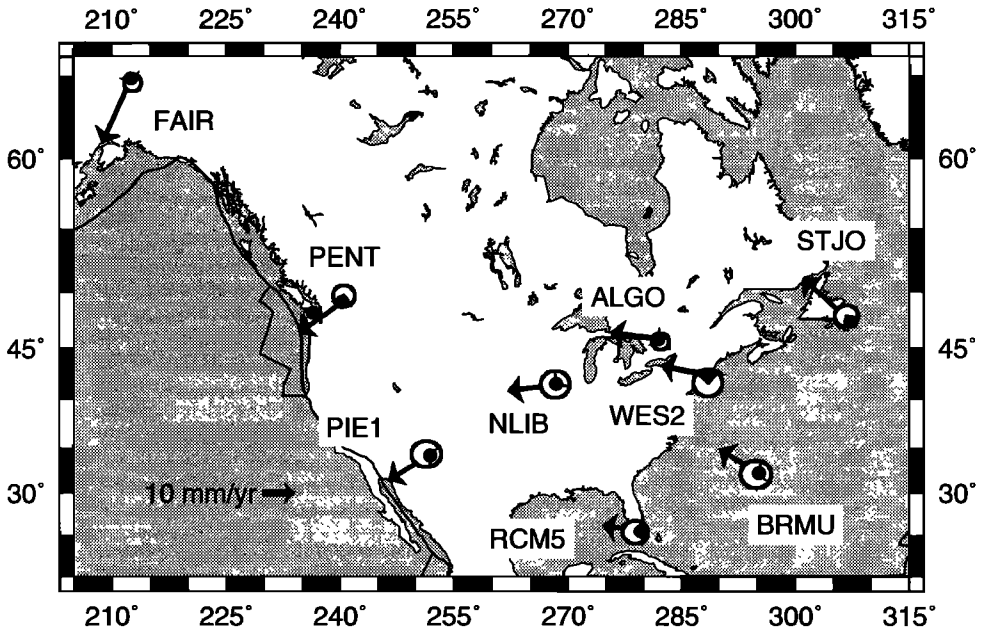

Figure 7. GPS station velocity estimates and NNR-A residuals for the North American plate. The 95% confidence regions are shown attached to the residuals. For clarity, the velocity and residual for Alberthead, British Columbia, are not shown.

good agreement with the previous analysis of *Argus and Heflin* [1995].

Our data do not show evidence of significant internal plate deformation, which agrees with an independent analysis of VLBI data by *Argus and Gordon* [1996]. We also see little evidence of vertical deformation from the GPS data. Algonquin rises 4.5±1.2 mm/yr, a consequence of the ITRF94 frame constraint. North Liberty (0.0±2.6 mm/yr), Richmond (−0.5±2.4 mm/yr), Westford (−0.4±2.7 mm/yr), and Bermuda (−1.3±2.9 mm/yr) all show no vertical deformation within one standard deviation. Our vertical estimate for North Liberty disagrees with the ITRF94 predicted subsidence of 13.5±2.8 mm/yr, which is based on VLBI observations. The resolution of this discrepancy will require a careful comparison by the VLBI and GPS analysis centers, although we note that our result is more plausible than the VLBI result and the difference could be explained by subsidence of the VLBI antenna.

Given the good agreement between predicted and observed velocities in stable North America, it is not surprising that the pole of rotation and angular speed also agree well with NNR-A. Our pole agrees with NNR-A to within 2° in pole position, well within one standard deviation.

Australia

Our analysis of Australian plate motion is based on the motions of five sites: Yaragadee, Canberra, Perth, Townsville, and Hobart. Yaragadee and Perth are located on the western coast, and Canberra and Hobart are located on the eastern coast and on the island of Tasmania, respectively. Of these, Yaragadee, Townsville, and Canberra were observed as early as GIG. Perth and Hobart came on-line with Rogue receivers in 1993. The Townsville site was abandoned for continuous observations in 1992, but we include it here for completeness. The locations of these sites and their velocities are shown in Figure 6. The size of the error ellipses reflects the time span of the observations. We find no discrepancies between NNR-A and the geodetic velocities at the 95% confidence limit. The baselines between the different Australian sites also show no significant lengthening or shortening, which is consistent with the NUVEL-1A assumption of no internal plate deformation.

The discrepancy between the NNR-A pole and our geodetic pole is 2.6° in latitude and 7.5° in longitude, with a maximum uncertainty of 3.1°. The Australia angular speed is smaller than predicted by NNR-A. Although the NNR-A pole discrepancy is not significant at 95% confidence, we have conducted several tests to determine the sensitivity of the Australia angular velocity to our data. For example, if we remove Yaragadee as a reference site and replace it by Canberra, the Australia pole is still shifted 7° east of the NNR-A pole. If we remove the Yaragadee or Canberra data from the angular velocity estimation, the pole moves less than 1° and the angular speed changes less than 0.01°/m.y. Fortunately, the Australian plate is well instrumented with GPS receivers and more accurate velocities should be available in a few years. Currently, the discrepancy between our angular velocity for Australia and NNR-A is not significant at the 95% confidence limit.

Also shown in Figure 6 is Wellington, New Zealand, located in the Pacific-Australian plate boundary zone.

A permanent GPS receiver was operated there throughout 1991-1992 and then was abandoned. Fortunately we have been able to augment our Wellington time series with campaign measurements taken in January 1994 and January 1995. Wellington's velocity is consistent with the plate boundary displacement field derived from terrestrial geodetic techniques by *Bibby et al.* [1986]. Our newly estimated velocity for Wellington agrees with that of *Larson and Freymueller* [1995] to better than 1 mm/yr and 2° in azimuth.

Pacific Plate

We have analyzed data from two continuous GPS sites on the Pacific plate: Kokee Park, Hawaii, and Pamatai, French Polynesia (Figure 6). We have a 5 year time series at Kokee Park and a 4 year time series at Pamatai. Kokee Park is a reference site and thus agrees better with ITRF94 than NNR-A. The resulting velocity for Kokee Park is 3 ± 1.5 mm/yr faster than NNR-A. The NNR-A velocity for Pamatai is 70.3 mm/yr, but our GPS velocity is 81.2 ± 2.9 mm/yr, about 15% faster. Initial SLR results for the nearby site at Huahine, French Polynesia, were reported as 87 ± 3 mm/yr [*Robbins et al.*, 1993] but have since been revised downward to 71 ± 3 mm/yr [*Boucher et al.*, 1996]. To expand our set of sites on the Pacific plate, we have also analyzed temporary and permanent data spanning 3.3 years from Chatham Island. The velocity of Chatham Island is about 20% faster than predicted by NNR-A. Velocities of all three are fit well by a pole of rotation that lies 11° (4σ) to the west of the NNR-A pole of rotation and has a angular speed greater by about 10% (6σ). The Pacific pole is the most precisely determined in our study because the GPS sites on the plate are so widely spaced.

No other plate in this study has an angular velocity so different from that predicted by NNR-A. To test our angular velocity, we use it to predict the velocities of SLR and VLBI sites on the Pacific plate. Our predicted velocities for Kwajalein (VLBI), and Maui (SLR) and Huahine (SLR) all agree with the ITRF94 velocities for those sites within the 95% confidence limits of the data. If we combine ITRF94 velocities for Kwajalein, Maui, and Huahine and our velocities from Pamatai and Chatham, the resulting pole is −63.3° latitude, 96.6° longitude, and the angular speed is 0.68°/m.y. We suggest that the motion of the Pacific plate over the last 5 years does not agree with its motion over the last 3 m.y.

Antarctica

There are two sites on the Antarctic plate that meet our criteria of a 2 year time span: McMurdo and O'Higgins. Both McMurdo and O'Higgins were observed during the GIG campaign. A permanent receiver was placed at McMurdo in February 1992 but has been moved twice since then. The permanent O'Higgins receiver was installed in early 1995. The differences between NNR-A predictions and our velocities for McMurdo (< 1 mm/yr) and O'Higgins (< 2 mm/yr) are remarkably small. The Antarctica pole agrees better with NNR-A in latitude than longitude, but the standard deviations are also larger in longitude than latitude. The prospects for future Antarctica measurements are good. Three additional sites on the Antarctica plate were added during 1994: Casey and Davis on the continent and Kerguelen Island. All of these sites are in the IGS network but were not installed early enough to contribute to this analysis.

Africa

The African plate is sampled at Hartebeesthoek, South Africa, and on the Canary Islands (Mas Palomas). The Mas Palomas velocity agrees with NNR-A to within 1 mm/yr. Hartebeestoek is one of our reference sites, so its velocity has been constrained to agree with ITRF94, and its agreement with NNR-A is only within three standard deviations. Since we do not have enough independent data from the African plate to evaluate the significance of the discrepancy at Hartebeesthoek, we cannot be sure that our estimate of African plate motion differs significantly from NNR-A. In any case, with only the two sites the angular velocity is not determined precisely, with an uncertainty of 7° in pole position longitude. Additional data from sites on the stable African plate are needed to improve the estimate of the angular velocity. At present, there is only one additional site on the African continent, and it has a short time history. This site (Malindi, Kenya) is located east of the East African Rift System, so it is not on the African plate. We expect it will be several years before a better estimate of African plate motion can be obtained.

Nazca

Sites on the Nazca plate are necessarily limited to islands. SLR measurements were made prior to the installation of a permanent GPS site on Easter Island in 1994. Our GPS velocity, shown in Figure 8, agrees at the two standard deviation level with both the NNR-A and the ITRF94 value. With only one site on the Nazca plate, we would be unable to estimate an angular velocity, so we have also included data from two temporary sites in the Galpagos Islands that were occupied as part of the Central and South America (CASA) experiment [*Freymueller et al.*, 1993]. We include data from Isla Baltra from 1991 and 1994, and data from a site on Isla Santa Cruz, about 30 km to the south, which was observed in 1994 and which became a permanent site in early 1996. The two sites are 30 km apart and were assumed to have the same velocity. The data are consistent with this assumption, and the 5 year time series yields a velocity that is significantly slower than NNR-A predictions. The difference between our velocity and the NNR-A prediction for that site is 20 ± 5 mm/yr (Figure 8). Our estimated pole of rotation for

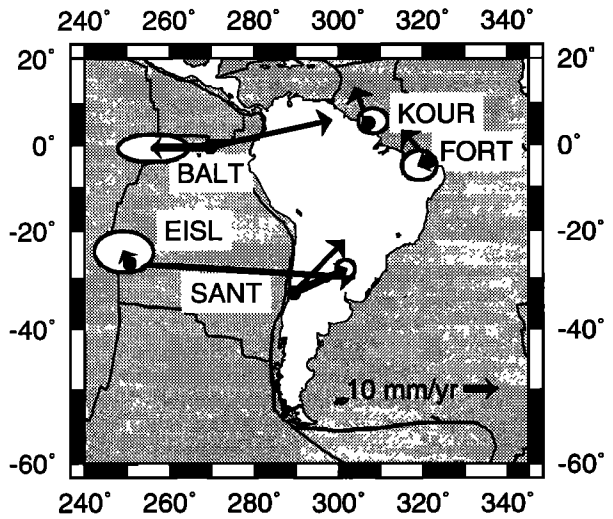

Figure 8. GPS station velocity estimates and NNR-A residuals for the South America and Nazca plates. The 95% confidence regions are shown attached to the residuals.

the Nazca plate differs by 8° from the NNR-A pole, but the uncertainty is almost as large (7°). A small shift in the pole position and angular speed can account for a large difference in velocity because the pole is located fairly close to the plate.

Previously published results for Baltra [*Freymueller et al.*, 1993] gave the motion of Baltra relative to Jerusalen in Ecuador based on data from 1988, 1990, and 1991. The 1990 and 1991 results for Baltra are consistent with the low rate obtained in this study, although the 1988 data are not. The 1988 CASA results also show an unexpected east-west movement of Baltra relative to Isla del Coco on the Cocos plate, which could be explained if the coordinates obtained for Baltra in 1988 were biased to the west. We conclude that the 1988 solutions for Baltra were probably biased and that the remaining data are consistent with a rate of motion much lower than predicted by NNR-A. Results from 1991 and 1994 for Isla Malpelo, about 800 km to the northeast of Baltra and also on the Nazca plate, are also consistent with a lower velocity than would be predicted by NNR-A. The motion of the Nazca plate is well constrained in the NUVEL-1A model since it is surrounded on three sides by spreading centers, so we would not expect NUVEL-1A to have an incorrect estimate of its motion. Active volcanism in the Galapagos Islands occurs about 75 km to the west, on Isabella and Fernandina islands [*Simkin and Siebert*, 1994]. Westward motion of both Galapagos Islands GPS sites could be caused by ongoing flexure of the lithosphere due to the load of the active volcanic islands if these islands were still subsiding today. However, we have no explanation that can definitively account for the entire discrepancy. It may be that the plate is deforming internally. Data from the Galapagos and Malpelo will be examined more fully in a future paper with the other CASA regional campaign data.

The large uncertainty in the pole position is controlled by the relatively large uncertainty in the velocity of Baltra. When the velocities of the Galapagos and Easter Island sites are determined with a precision of 1 mm/yr, these two sites will be sufficient to determine a precise pole of rotation (maximum pole uncertainty 2.5°), although data from additional sites would be required to determine whether the Nazca plate is deforming internally. Data from a regional campaign have been taken at a site in the Juan Fernandez islands in the southeast part of the Nazca plate, which may eventually help resolve this issue.

South America

We have analyzed data from three permanent GPS sites on the South American plate. Santiago is located in the South American/Nazca plate boundary zone. On the stable portion of the plate, we have observations from Fortaleza, Brazil, and Kourou, French Guyana. Their horizontal velocities and NNR-A discrepancy vectors are shown in Figure 8. Their velocities agree to better than 1 mm/yr with NNR-A in the north component and within two standard deviations in the east component.

The angular velocity for South America is the most poorly determined of the eight plates estimated in this paper. This is simply because Kourou and Fortaleza are less than 2000 km apart, yielding poor sensitivity to the longitude of the pole (maximum standard deviation of 31°). The addition of another site in southern South America would substantially improve the geometry for determining the pole of rotation. The uncertainty in the angular speed will be reduced by about 50% when the site in La Plata (near Buenos Aires) has a sufficiently precise velocity. The longitude of the pole will remain poorly constrained until a site in western South America, but east of the deforming Andes, is included. No permanent sites meeting that criterion have yet been established.

Relative Angular Velocity Vectors

Relative angular velocities describe the relative motions of a plate pair and can be derived by differencing the absolute angular velocities for the two plates. Angular velocities derived from GPS data are generally correlated, due to the correlations between sites in the GPS velocity field. Just as GPS relative velocities are more precise than absolute velocities, the uncertainties of relative plate angular velocities are smaller than those of absolute plate motions. Relative angular velocities are also less sensitive than absolute angular velocities to reference frame errors in the GPS velocities, or the no-net-torque assumption used to derive the NNR-A model from NUVEL-1A. We can compare our relative angular velocities directly with the NUVEL-1A relative plate motion model, and unlike NNR-A, standard deviations are available for NUVEL-1A. This allows us to

better assess the significance of discrepancies between the plate model predictions and our geodetic analysis.

In Table 6 we compare our relative angular velocity estimates to NUVEL-1A and other published geodetic studies. We have listed all plate pairs which share a boundary. For comparison with an independent GPS analysis, we list *Argus and Heflin* [1995] values when available (hereafter Jet Propulsion Laboratory (JPL)-GPS). Our study uses a longer time series than JPL-GPS, and includes more sites. We have also made a greater effort to augment our velocities by using data from temporary occupations of sites. The JPL-GPS paper also showed angular velocities derived from VLBI data, which they have made available (D. Argus and R. Gordon, manuscript in preparation, 1997) (hereafter VLBI). For comparison with a recent multiple-technique analysis, we list *Smith et al.* [1996] (hereafter Goddard). This group combined separate analyses of VLBI, SLR, GPS, and DORIS data to estimate angular velocities for many of the plates we discuss. The Goddard study has the advantage of having more data and more sites because they use several techniques, although inconsistencies between the velocity solutions used could potentially cause biases in the results. For several plates, they rely only on GPS data, and we expect good agreement of results for these plates.

We note two trends in Table 6. First of all, there is good agreement between nearly all our GPS derived relative angular velocities and NUVEL-1A, with the exception of some of those involving the Pacific plate. In general, there is also good agreement between the independent geodetic analyses, This is encouraging given that VLBI, SLR, DORIS, and GPS are quite distinct geodetic techniques and the data were analyzed and reference frame constraints applied in very different ways. The one exception to this good agreement is for the North America-Africa pole position. Upon closer inspection, it becomes clear that pole uncertainties are poorly defined at extremely high latitudes (the pole is located at a latitude of 79°). In this case, we have also inspected the Cartesian uncertainties, which indicate agreement with NUVEL-1A at better than two standard deviations.

In Table 7 we show the predicted relative motion at several locations along plate boundaries. Two angular velocities for a given plate pair may be significantly different and yet predict motions along the plate boundary that are not significantly different. This is the case for our Pacific-North America angular velocity, for example. Where our predicted relative motions on the plate boundary differ from those predicted by NUVEL-1A, we can compare our relative motions to the raw data from which NUVEL-1A is derived.

Eurasia-North America

In Figure 9, we show the pole position of the Eurasia-North American angular velocity. In each case, we have plotted the position and its 95% confidence ellipse. Our estimate agrees well with both NUVEL-1A and Goddard but has a relatively large uncertainty in the pole position estimate due to the poor geometry of the GPS sites on the Eurasian plate. The GPS-only solution will be improved when sites outside of western Europe contribute. The JPL-GPS and VLBI pole positions are located more northerly of NUVEL-1A. Our angular speed agrees with NUVEL-1A, as do all of the other geodetic solutions with the exception of the VLBI solution.

Pacific-North America

Pacific-North America relative plate motion has critical implications for deformation in the plate boundary zones of California and Alaska. Our estimated angular velocity (Figure 10) is significantly different than NUVEL-1A, both in pole location and angular speed. Our angular velocity disagrees with the other geodetic studies in longitude but agrees in latitude and rate. All of the geodetic techniques estimate a faster angular speed than NUVEL-1A, but only our rate and the VLBI rate exclude the NUVEL-1A rate from the 95% confidence region. The VLBI and Goddard angular velocities are based on different sets of stations. For VLBI, the sites are in the northern hemisphere, specifically Marcus Island, Hawaii, and Kwajalein. The GPS estimates are based on Hawaii and sites from the southern Pacific. The Goddard solution will average both northern and southern hemisphere as VLBI, SLR, and GPS data contribute to the angular velocity estimate. We are the only analysis listed in Table 6 which uses measurements from Chatham Island. Ongoing GPS measurements from sites such as Kwajalein and Chatham Island should resolve issues regarding the Pacific plate.

Despite the significant difference between our pole and the NUVEL-1A pole, both predict the same relative motion along almost the entire Pacific-North America plate boundary (Table 7). For a point in southern California near Vandenberg Air Force Base, we predict a relative plate motion vector of 46.4 ± 2.8 mm/yr toward N40.3°W±1.8, 2.7° westerly of NUVEL-1A but with the same rate to within 0.4 mm/yr. The azimuth difference is not significant at the two sigma level. In the Gulf of California, our model predicts relative motions 1.3 mm/yr faster than NUVEL-1A toward a direction 5.6° more westerly. The rate difference is insignificant, but the azimuth difference with NUVEL-1A is possibly significant. Our predicted rate and azimuth all well within the one sigma uncertainty range for spreading rates and transform fault azimuths in the Gulf of California, however [*DeMets et al.*, 1990]. *DeMets* [1995] showed that the 3.16 m.y. average spreading rate in the Gulf of California is slower than both the 0.78 m.y. average spreading rate and the NUVEL-1A closure-fitting rate (the Pacific-North America relative motion predicted by the NUVEL-1A data excluding data from that plate boundary), probably because the Gulf of California spreading centers did not accommodate the entire Pacific-North America relative motion until about 2 m.y. ago. Our

Table 6. Relative Angular Velocities for Plates Sharing a Boundary

Source	Angular Velocity			Pole Error Ellipse			
	Latitude, deg	Longitude, deg	ω, deg/m.y.	σ_{max}, deg	σ_{min}, deg	ψ deg	σ_ω, deg/m.y.
			Europe-North America				
This paper	68.1	126.6	0.24	6.5	3.9	−30	0.02
NUVEL-1A	62.4	135.8	0.21	4.1	1.3	−11	0.01
VLBI	74.0	111.3	0.26	5.4	2.4	−48	0.02
Goddard	66.7	126.8	0.22	3.0	1.2	−39	0.01
JPL-GPS	78.5	122.0	0.23	8.2	4.9	−8	0.03
			Pacific-North America				
This paper	−49.6	95.7	0.83	2.0	1.0	−86	0.02
NUVEL-1A	−48.7	101.8	0.75	1.3	1.2	61	0.01
VLBI	−50.5	104.1	0.78	2.0	0.8	−84	0.01
Goddard	−49.8	103.1	0.77	2.6	1.1	−86	0.02
JPL-GPS	−49.1	107.0	0.79	4.1	2.2	−83	0.03
			Africa-North America				
This paper	76.3	103.5	0.21	7.1	5.7	76	0.01
NUVEL-1A	78.9	38.3	0.24	3.8	1.0	77	0.01
Goddard	78.8	39.2	0.24	6.3	3.4	36	0.02
JPL-GPS	80.9	16.7	0.22	14.5	11.1	15	0.04
			South America-North America				
This paper	−11.1	126.7	0.29	6.6	3.9	27	0.08
NUVEL-1A	−16.4	121.9	0.15	6.2	3.9	9	0.01
JPL-GPS	-6.5	124.4	0.28	8.3	7.4	−55	0.12
			Pacific-Europe				
This paper	−61.5	90.0	0.97	2.1	0.9	-68	0.02
NUVEL-1A	−61.2	94.2	0.86	1.3	1.2	−90	0.02
Goddard	−61.9	98.4	0.90	2.4	0.8	−76	0.02
JPL-GPS	−60.2	95.6	0.95	3.3	2.2	-88	0.05
			Australia-Europe				
This paper	8.6	48.5	0.65	3.7	1.4	−46	0.02
NUVEL-1A	15.2	40.5	0.69	2.2	1.2	−45	0.01
Goddard	12.4	44.6	0.66	1.7	0.6	−51	0.02
JPL-GPS	9.9	47.4	0.72	4.9	4.0	−53	0.05
			Africa-Europe				
This paper	−23.5	−29.8	0.05	35.0	21.4	25	0.02
NUVEL-1A	21.2	−20.6	0.12	6.2	0.8	−4	0.02
Goddard	18.4	−24.6	0.10	13.3	10.0	−71	0.03
JPL-GPS	−11.7	−27.3	0.07	41.7	36.1	36	0.03
			Australia-Pacific				
This paper	65.7	2.9	1.04	1.7	1.5	2	0.02
NUVEL-1A	60.2	1.7	1.07	1.1	1.0	58	0.02
Goddard	60.8	3.9	1.07	1.9	1.0	29	0.02
JPL-GPS	57.2	6.5	1.13	2.6	2.4	43	0.04
			Antarctica-Pacific				
This paper	63.6	−95.0	0.93	2.0	1.5	44	0.03
NUVEL-1A	64.5	−84.0	0.87	1.2	1.1	82	0.01
Goddard	64.8	−82.3	0.90	2.7	1.7	84	0.06
			Africa-Australia				
This paper	−10.6	−127.3	0.65	3.3	1.9	58	0.02
NUVEL-1A	−12.5	−130.2	0.63	1.3	1.0	39	0.01
Goddard	−10.1	−127.0	0.63	2.5	1.8	−62	0.03
JPL-GPS	−11.2	−127.4	0.71	6.1	4.3	−22	0.04
			Antarctica-Australia				
This paper	−9.8	−136.8	0.65	4.4	2.6	20	0.01
NUVEL-1A	−13.2	−141.7	0.65	1.3	1.0	63	0.01
Goddard	−11.1	−138.6	0.64	5.2	2.5	30	0.03
LF	−12.8	−143.1	0.65	6.7	3.5	15	0.03
			South America-Africa				
This paper	−47.4	131.4	0.35	14.0	4.6	3	0.06
NUVEL-1A	−62.6	140.6	0.31	2.7	0.8	11	0.01
JPL-GPS	−39.9	131.7	0.38	16.2	7.4	−7	0.01
			Nazca-Pacific				
This paper	52.2	−94.5	1.37	4.2	1.4	2	0.04
NUVEL-1A	55.8	−90.1	1.36	1.9	0.9	−1	0.02
Goddard	67.3	−81.1	1.27	6.3	1.5	26	0.03

Table 6. (continued)

Source	Angular Velocity: Latitude, deg	Longitude, deg	ω, deg/m.y.	Pole Error Ellipse: σ_{max}, deg	σ_{min}, deg	ψ deg	σ_ω, deg/m.y.
			South America-Antarctica				
This paper	−63.75	126.5	0.29	20.2	4.4	6	0.05
NUVEL-1A	−86.44	139.3	0.26	3.1	1.2	24	0.01
			Africa-Antarctica				
This paper	-4.49	−42.5	0.11	24.2	13.8	3	0.02
NUVEL-1A	5.64	−39.2	0.13	4.6	1.4	−41	0.01
Goddard	5.6	−39.1	0.13	26.1	14.1	19	0.04
			Nazca-Antarctica				
This paper	30.0	−94.0	0.49	10.7	2.9	2	0.06
NUVEL-1A	40.7	−95.9	0.52	4.7	2.0	−9	0.02
Goddard	73.3	−77.0	0.37	21.4	4.1	−30	0.06
			South America-Nazca				
This paper	−43.8	95.2	0.74	9.1	5.5	18	0.07
NUVEL-1A	−56.1	86.0	0.72	3.7	1.5	10	0.02

NUVEL-1A from *DeMets et al.* [1990] and *DeMets et al.* [1994]; VLBI from D. Argus and R. Gordon (manuscript in preparation, 1997); Goddard from *Smith et al.* [1996]; JPL-GPS from *Argus and Heflin* [1995]; LF from *Larson and Freymueller* [1995]. Pole error ellipse convention defined as in Table 5

predicted spreading rate agrees almost exactly with the NUVEL-1A closure-fitting rate, and the 0.78 m.y. average spreading rate of *DeMets* [1995] lies within our one sigma uncertainty. At Kodiak Island in Alaska, our pole predicts relative motion 1.6 mm/yr more rapid and oriented 3.1° more northerly than NUVEL-1A; again, these differences are not significant. Only in the western Aleutians is our predicted Pacific-North America relative motion significantly different than NUVEL-1A, and there it is different in rate rather than azimuth. Since the only plate boundary data from the western Aleutians come from earthquake slip vectors, which are sensitive to the azimuth of relative plate motion, our faster rate of subduction here remains consistent with the available plate boundary data.

Pacific-Australia and Pacific-Eurasia

Unlike at the Pacific-North America plate boundary, our model predicts significantly different relative motion at both the Pacific-Australia and Pacific-Eurasia plate boundaries than NUVEL-1A. In these cases, relative plate motion on the boundary is significantly faster in our model but with the same azimuth as NUVEL-1A. Because both of these boundaries are subduction boundaries where the plate boundary data are sensitive to the azimuth of relative plate motions, our model is just as consistent with the data from those plate boundaries as is NUVEL-1A. No data from the Pacific-Australia plate boundary were used in determining NUVEL-1A. On the basis of the faster convergence rates predicted by our model, about 22% faster for the Pacific-Australia boundary and about 12% faster for the Pacific-Eurasia boundary, our data are consistent with a correspondingly higher rate of seismic moment release at these boundaries. Similar implications hold for the other plate boundaries in the western Pacific, including the Pacific-Philippine Sea plate boundary.

Table 7. Relative Plate Motions at Selected Locations on Plate Boundaries

Location	Latitude, deg	Longitude, deg	This study: Rate	This study: Azimuth	NUVEL1-A: Rate	NUVEL1-A: Azimuth
Vandenberg	34.6	−120.6	46.4±2.8	−40.3 ± 1.8	46.8±1.3	−37.6±1.5
Gulf of California	23.5	−108.5	48.7±2.8	−59.8 ± 2.0	47.4±1.2	−54.2±1.5
Kodiak, Alaska	57.6	−152.2	58.3±1.7	−18.3±2.5	56.7 ± 1.4	−21.4 ± 1.2
West Aleutians	51.0	173.1	79.4±1.7	−42.8±1.9	74.3±1.4	−45.6±0.9
Alpine fault, New Zealand	−43.5	170.0	45.4±1.7	−103.6±2.6	37.0±1.4	−109.1±2.1
Tokyo, Japan	36.1	140.1	103.4±2.6	−67.6±1.2	92.7±1.7	−69.0±0.9
East Pacific Rise	−10.0	−110.0	136.3±3.6	100.6 ± 1.4	139.9 ± 1.6	102.0±0.8
East Pacific Rise	−19.0	−113.0	145.5±3.6	101.8±1.3	147.4±1.5	103.0±0.8
East Pacific Rise	−30.0	−112.0	151.3±4.0	100.8±1.2	151.1±1.6	102.2±0.7

All rates are given in millimeters per year, and azimuths in degrees clockwise from north. Uncertainties are one standard deviation.

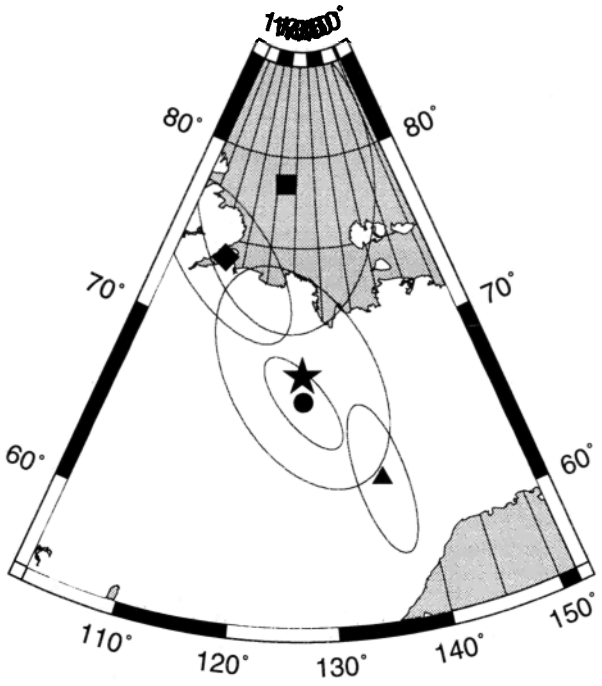

Figure 9. Eurasia-North American pole position, with 95% confidence region for *DeMets et al.* [1994] (triangle), *Smith et al.* [1996] (circle), VLBI (D. Argus and R. Gordon, manuscript in preparation, 1997) (square), *Argus and Heflin* [1995] (diamond), and this paper (star).

On the Alpine fault in New Zealand, our model predicts significantly faster relative plate motion, 8.4 mm/yr faster than NUVEL-1A and directed more obliquely to the trend of the Alpine fault. Projected onto the N55E trend of the Alpine fault, our velocity gives a fault-parallel rate of 42 mm/yr and a fault normal contraction rate of 16 mm/yr, compared to 36 mm/yr and 10 mm/yr for NUVEL-1A. The increased fault-normal contraction predicted by our model should be observable geodetically, and ongoing GPS observations in this area should be capable of testing our model prediction in the future. GPS results from the southwest Pacific [*Bevis et al.*, 1995; *Taylor et al.*, 1995] are consistent with our proposed Pacific-Australia convergence rate but are too imprecise to test the difference between our model prediction and NUVEL-1A.

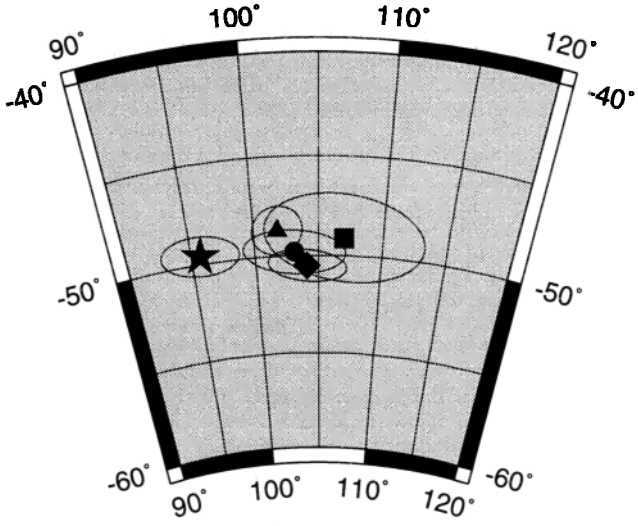

Figure 10. Pacific-North American pole position, with 95% confidence region for *DeMets et al.* [1994] (triangle), *Smith et al.* [1996] (circle), VLBI (D. Argus and R. Gordon, manuscript in preparation, 1997) (square), *Argus and Heflin* [1995] (diamond), and this paper (star).

The rate of underthrusting of the Pacific plate beneath the Japanese islands depends on both the Pacific-Eurasia relative plate motion and the motion of the Japanese islands relative to Eurasia, which we will not attempt to address here. At a location near Tokyo at the southern end of the main Japanese islands boundary with the Pacific plate, our model predicts 103.4±2.6 mm/yr of relative motion of the Pacific and Eurasian plates, 11.7 mm/yr faster than predicted by NUVEL-1A and oriented at the same azimuth within uncertainties.

Pacific-Nazca

Although our velocity for Baltra Island was significantly different than that predicted by NNR-A, the angular velocity for the Nazca plate agreed with NNR-A within its stated uncertainties. We have tested our Nazca-Pacific angular velocity by looking at predicted velocities at several locations along this plate boundary. As shown in Table 7, the agreement between NUVEL-1A and our model is very good. At −19.0° latitude, our model predicts 145.5±3.6 mm/yr at an azimuth of 101.8° ± 1.3°, whereas NUVEL-1A predicts 147.4±1.5 mm/yr. For the same location, *Wilson* [1993] finds a spreading rate of 153.7 mm/yr, slightly faster than our rate but within 95% confidence limits.

Antarctica-Australia

In Figure 11 we show the pole of rotation for Antarctica-Australia. There are no VLBI or SLR angular velocity estimates for the Antarctica plate. Goddard combined DORIS and GPS. For completeness, we compare our estimate with the *Larson and Freymueller* [1995] estimate for data that spanned 1991-1993. In that paper, the z component of the angular velocity was constrained to agree with NNR-A because there was only one site on the Antarctica plate. Our new estimate is based on the velocities of two sites on Antarctica, so there is no need to constrain the angular velocity. Again, the pole of rotation latitude agrees well between NUVEL-1A, Goddard, and our estimate. The angular speeds also agree within two standard deviations. The pole longitudes, as with Pacific-North America, agree less well.

Africa-Australia

The Africa Euler pole is not well determined by any of the geodetic techniques discussed in this paper, but the Africa-Australia relative angular velocity pole is relatively well determined. The NUVEL-1A standard de-

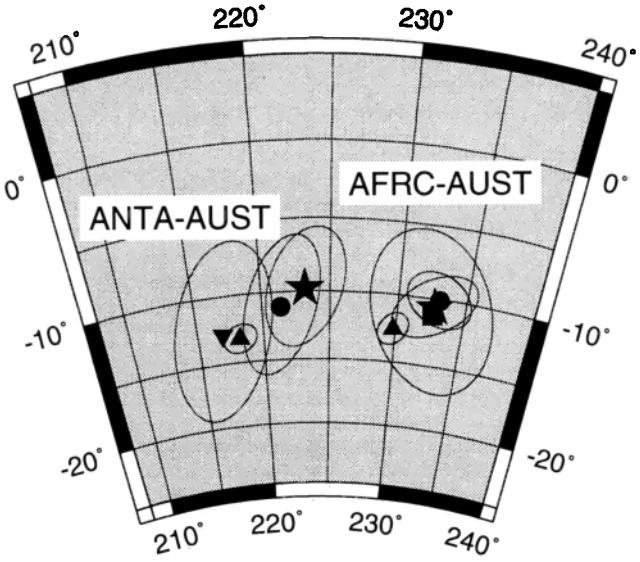

Figure 11. Antarctica-Australia and Africa-Australia pole positions, with 95% confidence region for *DeMets et al.* [1994] (triangle), *Argus and Heflin* [1995] (diamond), *Smith et al.* [1996] (circle), *Larson and Freymueller* [1995] (inverted triangle), and this paper (star).

viation for this plate pair is also quite small. Figure 11 shows that all the geodetic estimates agree within a few degrees, and all are offset from NUVEL-1A by 3°. The agreement between the different geodetic analyses is likely because all three are controlled by the GPS data from Mas Palomas and Hartebeesthoek. The discrepancy between NUVEL-1A and the geodetic analyses is most likely controlled by the GPS data from Hartebeesthoek, as discussed earlier.

North America-South America

Finally, we show a plate pair, North America-South America (Figure 12), for which there are no conventional plate motion data (i.e., seafloor spreading rates, transform fault azimuths, earthquake slip vectors). The NUVEL-1A pole uncertainty for this plate pair is as large as the geodetic standard deviation, as shown in Figure 12. The differences between our estimate, NUVEL-1A, and JPL-GPS are not significant at the 95% confidence limit.

Conclusions

In this paper, we have summarized the results for the analysis of a 5 year time span of global GPS data. We have concentrated on sites with long time histories, and for the most part, we have avoided sites in plate boundary zones. In several cases, we have been able to supplement continuous GPS measurements with earlier campaign style measurements, thus extending the time series by many years. We have also avoided sites contaminated with coseismic and postseismic deformation signals. We are thus able to compare GPS velocities with plate models, specifically the NUVEL-1A absolute plate motion model NNR-A. For all but a few sites, the agreement with NNR-A is better than 95% confidence. Specifically, sites in North America, Antarctica, South America, Eurasia, Africa, and Australia with long time series agree with NNR-A to better than 3 mm/yr. The discrepancies that do exist on the Pacific and Nazca plates are intriguing. GPS sites from the Pacific are faster than plate models would predict. In addition, sites in the south Pacific have larger discrepancies than sites in the north Pacific. On the Nazca plate, Baltra Island is almost 50% slower than NNR-A predictions. A nearby permanent GPS installation on the Galapagos Islands will be able to confirm this result within the next few years. For the most part, significant vertical deformation is limited to reference sites that required it or sites where we mixed permanent installations and campaigns (e.g., Wellington and Baltra). In these latter cases, antenna height recording errors can produce significant vertical error.

The data used in this analysis were available as the result of a cooperative international effort to install and operate GPS receivers throughout the world. With just 5 years of data, we were able to estimate angular velocities for eight tectonic plates. Continued expansion of the IGS network should allow for angular velocity estimation for most of the remaining tectonic plates by the end of the century. We currently assume that all site velocities vary linearly in time. With extension of these time series, we will be able to address the validity of that assumption, as well as investigating the significance of vertical deformation.

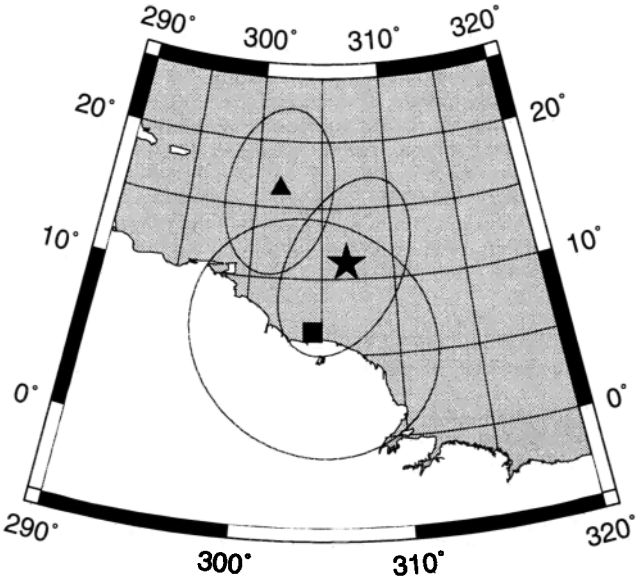

Figure 12. North America-South America angular velocity pole position, with 95% confidence region for *DeMets et al.* [1994] (triangle), *Argus and Heflin* [1995] (diamond), and this paper (star).

Acknowledgments. This research was funded by NASA NAG5-1908. We are grateful to many organizations and individuals for providing data and software support, including Zuheir Altamimi, John Beavan, Geoff Blewitt, Yehuda Bock, Claude Boucher, James Campbell, Chuck DeMets, Carey Noll, Andreas Reinhold, Wolfgang Schlueter, Teresa Van Hove, and JPL section 335. We thank Don Argus, Richard Gordon, Michael Heflin, Jim Ray, John Robbins, and George Rosborough for helpful discussions and providing us with their current results. Chuck DeMets and Richard Gordon made many helpful suggestions for improvement of the manuscript. This study would not have been possible without the development of the IGS. Plate models described in this paper may be viewed at http://spot.colorado.edu/kristine/jgr.plates.html.

References

Argus, D., Postglacial rebound from VLBI geodesy: On establishing vertical reference, *Geophys. Res. Lett., 23,* 973-976, 1996.

Argus, D., and R. Gordon, Pacific North American plate motion from very long baseline interferometry compared with motion inferred from magnetic anomalies, transform faults, and earthquake slip vectors, *J. Geophys. Res., 95,* 17,315-17,324, 1990.

Argus, D., and R. Gordon, No-net rotation model of current plate velocities incorporating plate motion model NUVEL-1, *Geophys. Res. Lett., 18,* 2039-2042, 1991.

Argus, D., and R. Gordon, Test of the rigid-plate hypothesis and bounds on intraplate deformation using geodetic data from very long baseline interferometry, *J. Geophys. Res., 101,*13,555-13,572, 1996.

Argus, D. and M. Heflin, Plate motion and crustal deformation estimated with geodetic data from the Global Positioning System, *Geophys. Res. Lett., 22,* 1973-1976, 1995.

Bar-Sever, Y. E., A new model for GPS yaw attitude, in *Proceedings, IGS Workshop: Special Topics and New Directions,* edited by G. Gendt and G. Dick, pp. 128-140, GeoForschungsZentrum, Potsdam, Germany, 1996.

Beutler, G., I. Bauersima, W. Gurtner, M. Rothacher, T. Schildknecht, G. L. Mader, and M.D. Abell, Evaluation of the 1984 Alaska Global Positioning System campaign with the Bernese GPS software, *J. Geophys. Res., 92,* 1295-1303, 1987.

Bevis, M. et al., Geodetic observations of very rapid convergence and back-arc extension at the Tonga arc, *Nature, 374,* 249-251, 1995.

Bibby, H.M., A.J. Haines, and R.I. Walcott, Geodetic strain and the present day plate boundary zone through New Zealand, *Bull. R. Soc. N.Z., 24,* 427-438, 1986.

Bierman, G.J., *Factorization Methods for Discrete Sequential Estimation, Math. Sci. Eng. Ser.*, vol. 128, Academic, San Diego, Calif., 1977.

Blewitt, G., Carrier phase ambiguity resolution for the Global Positioning System applied to geodetic baselines up to 2000 km, *J. Geophys. Res., 94,*10,187-10,203, 1989.

Blewitt, G., An automatic editing algorithm for GPS data, *Geophys. Res. Lett., 17,* 199-202, 1990.

Blewitt, G., M. Heflin, W. Bertiger, F. Webb, U. Lindqwister, and R. Malla, Global coordinates with centimeter accuracy in the international terrestrial reference frame using the Global Positioning System, *Geophys. Res. Lett., 19,* 853-856, 1992.

Bock, Y., Analysis of continuous GPS measurements in the Los Angeles Basin: Techniques and initial results, *Eos Trans. AGU, 76*(46), Fall Meet. Suppl., F141, 1995.

Boucher, C., Z. Altamimi, and L. Duhem, ITRF 92 and its associated velocity field, *IERS Tech. Note 15,* IERS Cent. Bur., Obs. de Paris, 1993.

Boucher, C., Z. Altamimi, and L. Duhem, Results and analysis of the ITRF 93, *IERS Tech. Note 18,* IERS Cent. Bur., Obs. de Paris, 1994.

Boucher, C., Z. Altamimi, M. Feissel, and P. Sillard, Results and analysis of the ITRF 94 , *IERS Tech. Note 20,* IERS Cent. Bur., Obs. de Paris, 1996.

Clark, T.A., D. Gordon, W.E. Himwich, C. Ma, A. Mallama, and J.W. Ryan, Determination of relative site motions in the western United States using Mark III very long baseline interferometry, *J. Geophys. Res. 92,* 12,741-12,750, 1987.

Chase, C.G., The n-plate problem of plate tectonics, *Geophys. J. R. Astron. Soc., 29,* 117-122, 1972.

Chase, C.G., Plate kinematics: The Americas, East Africa, and the rest of the world, *Earth Planet. Sci. Lett., 37,* 355-368, 1978.

DeMets, C., A reappraisal of seafloor spreading lineations in the Gulf of California: Implications for the transfer of Baja California to the Pacific plate and estimates of Pacific-North America motion, *Geophys. Res. Lett., 22,* 3345-3348, 1995.

DeMets, C., R. Gordon, D. Argus, and S. Stein, Current plate motions, *Geophys. J. Int., 101,* 425-478, 1990.

DeMets, C., R. Gordon, D. Argus, and S. Stein, Effect of recent revisions to the geomagnetic reversal time scale on estimates of current plate motions, *Geophys. Res. Lett., 21,* 2191-2194, 1994.

Dong, D. and Y. Bock, GPS network analysis with phase ambiguity resolution applied to crustal deformation studies in California, *J. Geophys. Res., 94,* 3949-3966, 1989.

Fliegel, H. F, T. E. Gallini, and E.R. Swift, Global Positioning System radiation force model for geodetic applications, *J. Geophys. Res., 97,* 559-568, 1992.

Freymueller, J., J. Kellogg, and V. Vega, Plate motions in the North Andean region, *J. Geophys. Res., 98,* 21,853-21,863, 1993.

Heflin, M. et al., Global geodesy using GPS without fiducial sites, *Geophys. Res. Lett., 19,* 131-134, 1992.

Herring, T.A., Correlated noise processes in VLBI and GPS measurements, *Eos Trans AGU 77*(17), Spring Meet. Suppl., S69, 1996.

Herring, T. A., D. Dong, and R.W. King, Sub-milliarcsecond determination of pole position using Global Positioning System data, *Geophys. Res. Lett., 18,* 1893-1896, 1991.

Hofmann-Wellenhof, B., H. Lichtenegger, and J. Collins, *GPS: Theory and Practice,* Springer-Verlag, New York, 1993.

King, N.E., J. L. Svarc, E.B. Fogelman, W.K. Gross, K.W. Clark, G.D. Hamilton, C.H. Stiffler, and J.M. Sutton, Continuous GPS observations across the Hayward fault, California, 1991-1994, *J. Geophys. Res., 100,* 20,271-20,284, 1995.

Langbein, J., and H. Johnson, Correlated errors in geodetic time series: Implications for time-dependent deformation, *J. Geophys. Res., 102,* 591-603, 1997.

Larson, K.M., and J. Freymueller, Relative motions of the Australian, Pacific, and Antarctic plates using the Global Positioning System, *Geophys. Res. Lett., 22,* 37-40, 1995.

LePichon, X., Sea-floor spreading and continental drift, *J. Geophys. Res., 73,* 3661-3697, 1968.

Leick, A., *GPS Satellite Surveying,* 2nd ed., Wiley-Interscience, New York, 1995.

Lichten, S., and J. Border, Strategies for high precision Global Positioning System orbit determination, *J. Geophys. Res., 92,* 12,751-12,762, 1987.

Melbourne, W. G., S. S. Fisher, R. E. Neilan, T. P. Yunck,

B. Engen, C. Reigber, and S. Tatevjan, The first GPS IERS and geodynamics experiment - 1991, in *Permanent Satellite Tracking Networks for Geodesy and Geodynamics, IAG Symp.* vol. 109, edited by G. L. Mader, pp. 65-80, Springer-Verlag, New York, 1993.

Minster, J. B., and T.H. Jordan, Present-day plate motions, *J. Geophys. Res., 83,* 5331-5354, 1978.

Minster, J. B., T.H. Jordan, P. Molnar, and E. Haines, Numerical modeling of instantaneous plate tectonics, *Geophys. J. R. Astron. Soc., 36,* 541-576, 1974.

Molnar, P., and J. M. Gipson, A bound on the rheology of continental lithosphere using very long baseline interferometry: The velocity of South China with respect to Eurasia, *J. Geophys. Res., 101,* 545-554, 1996.

Robbins, J. W., D. E. Smith, and C. Ma, Horizontal crustal deformation and large scale plate motions inferred from space geodetic techniques, in *Contributions of Space Geodesy to Geodynamics: Crustal Dynamics, Geodyn. Ser.*, vol. 23, edited by D.E. Smith and D.L. Turcotte, pp. 21-36, AGU, Washington D.C., 1993.

Ryan, J. W., T. A. Clark, C. Ma, D. Gordon, D. Caprette, and W. Himwich, Global scale tectonic plate motions measured with CDP VLBI data, in *Contributions of Space Geodesy to Geodynamics: Crustal Dynamics, Geodynam. Ser.*, vol. 23, edited by D.E. Smith and D.L. Turcotte, pp. 37-49, AGU, Washington D.C., 1993.

Schupler, B., and T. Clark, How different antennas affect the GPS observable, *GPS World, 2,* 32-36, 1991.

Simkin, T., and L. Siebert, *Volcanoes of the World,* 349 pp., 2nd ed., Geoscience Press, Tucson, Ariz., 1994.

Smith, D. E., R. Kolenkiewicz, P.J. Dunn, J.W. Robbins, M.H. Torrence, S.M. Klosko, R.G. Williamson, E.C. Pavlis, N.B. Douglas, and S.K. Fricke, Tectonic motion and deformation from satellite laser ranging to LAGEOS, *J. Geophys.Res., 95,* 22,013-22,041, 1990.

Smith, D. E., R. Kolenkiewicz, J.W. Robbins, P.J. Dunn, M.H. Torrence, M. Heflin, and L. Soudarin, A space geodetic plate motion model, *Eos Trans. AGU, 77,* (17), Spring Meet. Suppl., S73, 1996.

Taylor, F. W. et al., Geodetic measurements of convergence at the New Hebrides island arc indicate fragmentation caused by an impinging aseismic ridge, *Geology, 23,* 1011-1014, 1995.

Tralli, D., T. Dixon, and S. Stephens, The effect of wet tropospheric path delays on estimation of geodetic baselines in the Gulf of California using the Global Positioning System, *J. Geophys. Res., 93,* 6545-6557, 1988.

Wilson, D. S., Confirmation of the astronomical calibration of the magnetic polarity timescale from sea-floor spreading rates, *Nature, 364,* 788-790, 1993.

J. T. Freymueller, Geophysical Institute, University of Alaska, Fairbanks, AK 99775. (e-mail: jeff@giseis.alaska.edu)

K. M. Larson and S. Philipsen, Department of Aerospace Engineering Sciences, University of Colorado, Boulder, CO 80309. (e-mail: kristine.larson@colorado.edu; philipse@lemond.colorado.edu)

(Received August 2, 1996; revised January 31, 1997; accepted February 6, 1997.)